Pathways for CO_2 formation and conversion during Fischer–Tropsch synthesis on iron-based catalysts

Sundaram Krishnamoorthy, Anwu Li, and Enrique Iglesia *

Department of Chemical Engineering, University of California, Berkeley, CA 94720, USA

Received 20 November 2001; accepted 31 January 2002

CO_2 reaction and formation pathways during Fischer–Tropsch synthesis (FTS) on a co-precipitated Fe–Zn catalyst promoted with Cu and K were studied using a kinetic analysis of reversible reactions and with the addition of ^{13}C-labeled and unlabeled CO_2 to synthesis gas. Primary pathways for the removal of adsorbed oxygen formed in CO dissociation steps include reactions with adsorbed hydrogen to form H_2O and with adsorbed CO to form CO_2. The H_2O selectivity for these pathways is much higher than that predicted from WGS reaction equilibrium; therefore readsorption of H_2O followed by its subsequent reaction with CO-derived intermediates leads to the net formation of CO_2 with increasing reactor residence time. The forward rate of CO_2 formation increases with increasing residence time as H_2O concentration increases, but the net CO_2 formation rate decreases because of the gradual approach to WGS reaction equilibrium. CO_2 addition to synthesis gas does not influence CO_2 forward rates, but increases the rate of their reverse steps in the manner predicted by kinetic analyses of reversible reactions using non-equilibrium thermodynamic treatments. Thus the addition of CO_2 could lead to the minimization of CO_2 formation during FTS and to the preferential removal of oxygen as H_2O. This, in turn, leads to lower average H_2/CO ratios throughout the catalyst bed and to higher olefin content and C_{5+} selectivity among reaction products. The addition of $^{13}CO_2$ to $H_2/^{12}CO$ reactants did not lead to significant isotopic enrichment in hydrocarbon products, indicating that CO_2 is much less reactive than CO in chain initiation and growth. We find no evidence of competitive reactions of CO_2 to form hydrocarbons during reactions of $H_2/CO/CO_2$ mixtures, except *via* gas phase and adsorbed CO intermediates, which become kinetically indistinguishable from CO_2 as the chemical interconversion of CO and CO_2 becomes rapid at WGS reaction equilibrium.

KEY WORDS: CO_2 formation; Fischer–Tropsch synthesis; iron-based catalysts.

1. Introduction

The Fischer–Tropsch synthesis (FTS) converts synthesis gas mixtures derived from coal or natural gas into useful fuels and petrochemicals [1–5]. Fe-based materials catalyze this reaction without loss of selectivity or catalyst damage over a wider range of reaction conditions than Co-based catalysts. Fe catalysts also give higher selectivity to olefins and alcohols than Co catalysts. Structural and chemical promoters (*e.g.* SiO_2, ZnO, CuO, K_2CO_3) are typically present in Fe-based catalysts and these promoters influence their surface areas, the extent to which oxide precursors convert to Fe carbides, and the rate of undesired side reactions. Our previous studies have probed the role of these promoters on the structure and function of catalysts prepared from Fe–Zn oxide precursors [6–8]. Zn is present as $ZnFe_2O_4$ and inhibits sintering of Fe oxides during thermal treatments [7]. CuO and K_2CO_3 increase reduction and carburization rates during the activation of the oxide precursors in synthesis gas and lead to higher active surface areas and to a larger number of active sites [6–8]. Potassium also titrates residual acid and hydrogenation sites and increases olefin content and product molecular weight [4,7,9,10].

* To whom correspondence should be addressed.
E-mail: iglesia@cchem.berkeley.edu

The removal of chemisorbed oxygen atoms (O^*) formed in the CO dissociation steps required for monomer formation during FTS can occur *via* reactions of O^* with co-adsorbed hydrogen (H^*) or carbon monoxide (CO^*). These reactions lead to the formation of H_2O and CO_2, respectively, as the oxygen carrier. In this manner, H_2O and CO_2 both form as primary FTS products. CO_2 and H_2O can also form *via* secondary reactions, but thermodynamic constraints lead to the net formation of CO_2 and the net depletion of H_2O at typical FTS reaction conditions. This occurs with the overall stoichiometry of the water–gas shift (WGS) reactions on Fe-based FTS catalysts [5,11,12]. Fe, Zn and Cu oxides can also provide active sites for these CO_2-forming reactions [11–13], which are useful for coal-derived synthesis gas streams ($H_2/CO \approx 0.7$), because oxygen rejection by excess CO reactants allows more efficient use of these CO-rich streams. For synthesis gas streams derived from natural gas, CO_2 formation leads to high H_2/CO ratios along the reactor bed and to lower olefin and C_{5+} selectivities. The control of oxygen removal *via* both primary removal and secondary oxygen removal pathways remains a critical issue in the design and use of Fe-based catalysts for FTS reactions.

The mechanism of CO_2 formation and the role of CO_2 in chain growth remain controversial. Some studies propose that FTS and WGS reactions proceed on different

1011-372X/02/0500-0077/0

sites [13–15] with carbide sites involved in FTS and Fe_3O_4 as the active phase for WGS reactions involving surface formate ($HCOO^*$) intermediates [16]. The rapid dynamic interconversion between FeC_x and Fe_3O_4 during FTS [8] makes the site assignments for these two reactions difficult to support with definitive experimental evidence. Most studies, however, do not consider primary CO_2 formation routes at all during FTS. The non-zero CO_2 selectivity observed at low CO conversions and low H_2O concentrations, and the expected presence of O^* and CO^* during FTS, show that CO_2 can also form as a primary product. Yet another CO_2 formation route involves the synthesis and decomposition of organic acids [17–19]. CO_2 can form *via* decarboxylation of organic acids formed from FTS alcohol products. The addition of $^{14}CH_3OH$ [17] or 1-pentanol [1-^{14}C] [18] to $H_2/^{12}CO$ led to higher ^{14}C contents in CO_2 than in CO, suggesting an intermediate role of alcohols in CO_2 formation. The absence of ^{14}C in C_1–C_4 products during the addition of 1-pentanol [1-^{14}C] suggests that CO_2 is not formed *via* direct alcohol decomposition, but rather *via* oxidation of alcohol to carboxylic acids followed by subsequent decarboxylation to form CO_2 and an olefin [18].

Another important aspect of CO_2 chemistry during FTS is its potential role in monomer formation and chain initiation. The addition of $^{14}CO_2$ (1.4 mol%) to $H_2/^{12}CO$ (1:1) did not lead to detectable ^{14}C contents on fused Fe catalysts (501 K, 0.1 MPa, $H_2/CO = 1$) [19]. More recent studies by Xu *et al.* [20,21], however, detected almost identical radioactivity per mole in CO_2 and in hydrocarbons on an Fe–Si–K catalyst (543 K, 0.8 MPa, $H_2/CO = 0.7$), suggesting that each hydrocarbon molecule contained one ^{14}C from $^{14}CO_2$. These latter results are surprising in view of the isotopic and chemical equilibration detected between CO and CO_2 in the effluent stream, which would render the chemical source of the carbon atoms indeterminate.

Here, we describe the role of CuO and K_2CO_3 promoters on primary and secondary CO_2 formation pathways during FTS and probe the relative rates of primary oxygen removal *via* reaction with adsorbed hydrogen (to form H_2O) or with adsorbed CO (to form CO_2). $^{13}CO_2$ addition studies at conditions far from water–gas shift equilibrium are used to show that CO_2 is essentially inert in chain growth or initiation reactions and that its chemical conversion to hydrocarbons occurs *via* surface or gas phase CO intermediates. Finally, a reversible reaction kinetic analysis approach is developed in order to describe the effects of CO_2 recycle on CO_2 selectivity. As suggested previously [9], the presence of CO_2 inhibits the net rate of WGS during FTS on Fe-based catalysts. The addition or recycle of CO_2 decreases the net rate of CO_2 formation and increases the fraction of the oxygen atoms in CO removed as H_2O, an important practical issue in the use of Fe-based catalysts for H_2/CO mixtures derived from natural gas.

2. Experimental methods

All catalysts were prepared by co-precipitation from a solution containing Zn and Fe nitrates at a constant pH of 7.0 to form Fe–Zn oxides, which were then impregnated to incipient wetness with aqueous solutions of copper nitrate and potassium carbonate [6,7]. These catalysts are denoted as $FeZn_{0.1}$, $FeZn_{0.1}Cu_{0.01}$, $FeZn_{0.1}K_{0.02}$ and $FeZn_{0.1}K_{0.02}Cu_{0.01}$; the subscripts give the atomic ratios for each promoter relative to Fe. $^{13}CO_2$ addition experiments were carried out on a high surface area $FeZn_{0.1}K_{0.04}Cu_{0.02}$ catalyst synthesized using previously reported procedures [7], which lead to very high catalytic activity by exploiting the use of surface-active alcohol additives in order to prevent loss of surface area during drying of Fe–Zn oxide precursors.

Fischer–Tropsch synthesis rates and selectivities were measured in a single-pass packed-bed reactor with plug-flow hydrodynamics (1.125 cm diameter, SS-304); this reactor was held within a resistively heated three-zone furnace (ATS 302C Series 3210). Catalyst samples (0.4 g, 100–180 μm) were diluted with ground quartz ($\sim$11 g, 100–180 μm) in order to prevent reactor temperature gradients caused by the exothermic FTS reactions. Axial temperatures were measured using a movable thermocouple; they were within $\pm$0.5 K of the average temperature along the entire bed length. Synthesis gas ($H_2/CO/N_2$ 62/31/7, Praxair, N_2 internal standard) was purified using carbonyl (Sorb-Tech RL-13, activated carbon) and water (Matheson 452 A, 4 Å sieve) removal traps. An equimolar $^{12}CO_2$/Ar mixture (Linde, Air Products Co.) was used in $^{12}CO_2$ addition experiments carried out to simulate recycle conditions. The pressure of $^{12}CO_2$ was varied while maintaining a constant synthesis gas pressure. The system pressure was controlled using a dome-loaded regulator (Mity Mite Model S-91xw). All transfer lines after the reactor were kept at 433–453 K in order to prevent condensation of C_1–C_{15} products. $^{13}CO_2$ addition experiments were carried out in order to probe the role of CO_2 in chain initiation and growth by adding 0.1 MPa $^{13}CO_2$ (Cambridge Isotope Laboratories Inc., 99% isotopic purity) at 508 K, 0.8 MPa synthesis gas pressure, and an H_2/CO ratio of 2.0.

Reactant and effluent streams were analyzed using on-line gas chromatography (Hewlett-Packard, Model 5890 Series II). C_1–C_{15} hydrocarbon concentrations were measured by direct sampling of the effluent stream using a flame ionization detector and a methyl silicone capillary column (Hewlett-Packard HP-1, 50 m $\times$ 0.32 mm $\times$ 1.05 μm). Fixed gases and CH_4 were analyzed using a thermal conductivity detector and a Porapak Q packed column (15.2 cm $\times$ 0.318 cm). The ^{13}C content in the products of $^{13}CO_2/^{12}CO/H_2$ mixtures was measured using a mass selective detector (Hewlett-Packard, Model 5890; Series II/5791A) and separating the products with an HP-1 capillary column (cross-linked methyl silicone,

50 m × 0.32 mm × 1.05 μm). The ^{13}C contents in reactants and products were measured from mass ion intensities using deconvolution techniques that account for natural abundance and mass fragmentation patterns [22].

Promoted Fe–Zn oxide precursors were activated within the FTS reactor using synthesis gas (0.1 MPa) by increasing the temperature from 293 K to 543 K at a rate of 0.017 K/s. After synthesis gas reactions at 543 K for 0.5 h, the reactor temperature and pressure were set to the desired conditions and sampling of the effluent continued until product concentrations reached steady-state.

3. Results and discussion

3.1. Role of CuO and K_2CO_3 promoters on CO_2 formation pathways

CO_2 selectivities on $FeZn_{0.1}$, $FeZn_{0.1}Cu_{0.01}$, $FeZn_{0.1}K_{0.02}$ and $FeZn_{0.1}K_{0.02}Cu_{0.01}$ are shown as a function of CO conversion for stoichiometric synthesis gas ($H_2/CO = 2$) at 508 K and 2.14 MPa in figure 1(a) and at 543 K and 0.5 MPa in figure 1(b). These data were obtained by changing the CO space velocity at constant temperature and H_2 and CO partial pressures. CO_2 selectivities increased with decreasing space velocity (and increasing reactor residence time and CO conversion) on all catalysts. This increase in CO_2 selectivity reflects the formation of CO_2 by reactions of water with CO-derived intermediates in secondary reactions with the stoichiometry of the water–gas shift reaction. In these reactions, H_2O formed in primary oxygen removal steps readsorbs on sites where it can dissociate and its extent of readsorption and reaction increases, as the concentration of water increases with increasing CO conversion and decreasing space velocity. The dependence of CO_2 selectivity on reactor residence time weakens at higher CO conversion levels, as CO_2-forming reactions approach equilibrium on all catalysts.

CO_2 selectivities are higher on promoted Fe catalysts than on unpromoted samples at all CO conversion levels. The slope of these CO_2 selectivity curves at different points (figure 1) (or more rigorously the slopes of the CO_2 formation rates shown later) gives a measure of the rate of secondary CO_2-forming reactions. These slopes are very similar for $FeZn_{0.1}K_{0.02}$ and $FeZn_{0.1}K_{0.02}Cu_{0.01}$ catalysts at 508 K (figure 1(a)). Similarly, $FeZn_{0.1}$ and $FeZn_{0.1}Cu_{0.01}$ catalysts also show nearly identical slopes, indicating that the addition of Cu to $FeZn_{0.1}K_{0.02}$ or $FeZn_{0.1}$ does not increase the rate of WGS reactions. Figures 2(a) and 2(b) show the oxygen selectivities to H_2O on all four catalysts at the two reaction conditions of this study. This oxygen selectivity is defined as the percentage of the oxygen in the converted CO that appears as a given product, in the case of figure 2 as H_2O. The oxygen selectivity to H_2O decreases with increasing CO conversion as water readsorbs and finds additional opportunities to react and approach equilibrium, which favors CO_2 as the oxygen removal carrier at these reaction conditions. These H_2O selectivities extrapolate to high values as CO conversion decreases, consistent with a high primary selectivity for oxygen removal as water. The readsorption of water, and its subsequent probability of reaction with CO-derived intermediates to form CO_2, leads to a decrease in the H_2O selectivity with increasing CO conversion (figure 2).

The CO_2 selectivities extrapolated to low CO conversion levels are non-zero, consistent with these primary pathways for oxygen removal as both CO_2 and H_2O. Cu increases this primary selectivity to CO_2 and thus the propensity for O^* removal as CO_2 on Fe–Zn catalysts. In contrast, K increases the rate of the secondary WGS reaction without influencing primary CO_2 selectivities (figures 1 and 2). It appears that K promotion does not influence the relative abundance of CO^* and H^* species available for oxygen removal, even though

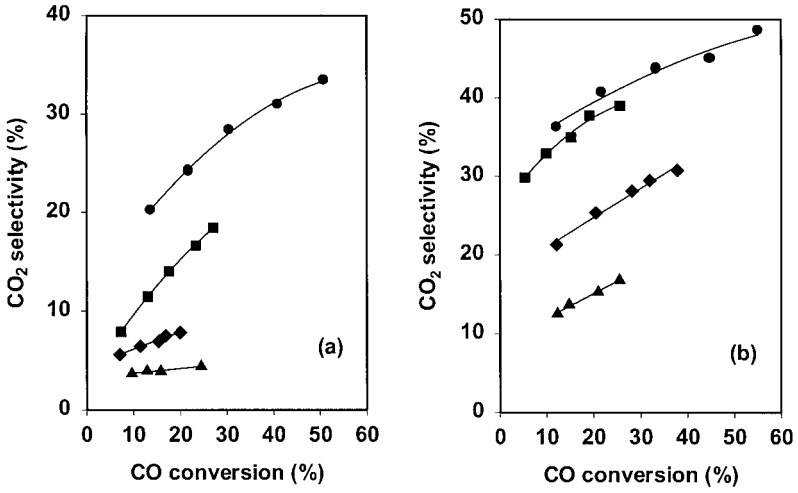

Figure 1. CO_2 selectivity as a function of CO conversion on the different Fe catalysts at (a) 508 K, 2.14 MPa, $H_2/CO = 2$, and (b) 543 K, 0.5 MPa, $H_2/CO = 2$. (▲): $FeZn_{0.1}$, (◆): $FeZn_{0.1}Cu_{0.01}$, (■): $FeZn_{0.1}K_{0.02}$, and (●): $FeZn_{0.1}K_{0.02}Cu_{0.01}$.

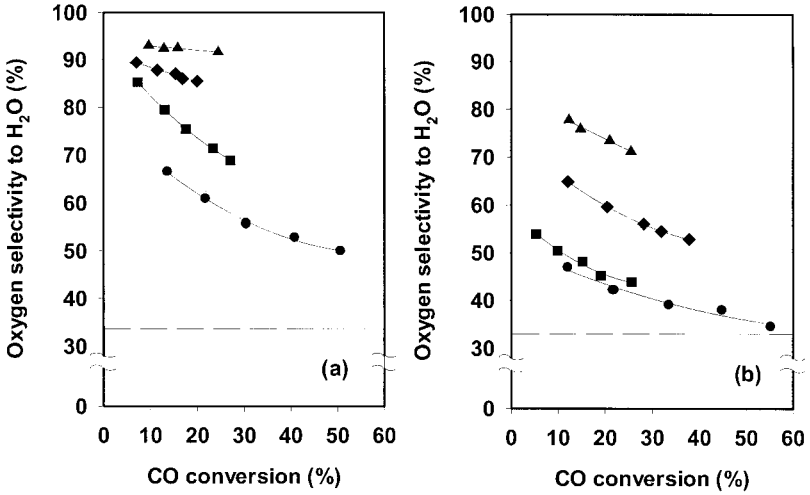

Figure 2. Oxygen selectivity to H_2O as a function of CO conversion on the different Fe catalysts at (a) 508 K, 2.14 MPa, $H_2/CO = 2$, and (b) 543 K, 0.5 MPa, $H_2/CO = 2$. (▲): $FeZn_{0.1}$, (◆): $FeZn_{0.1}Cu_{0.01}$, (■): $FeZn_{0.1}K_{0.02}$, and (●): $FeZn_{0.1}K_{0.02}Cu_{0.01}$. Dashed line: oxygen selectivity to H_2O at WGS equilibrium.

previous studies have suggested that the effects of K on hydrocarbon selectivity and FTS rates reflect an increase in the binding energy of adsorbed CO relative to that of hydrogen [4,9]. The higher CO_2 selectivity on Cu-containing catalysts suggests that Cu increases the availability of CO^* for O^* removal in primary pathways, but that Cu does not increase the rate of secondary CO_2-forming reactions (see slopes in figure 1), even though previous reports have attributed higher CO_2 selectivities on Cu-promoted samples to Cu-catalyzed WGS reactions [23]. The primary CO_2 selectivity is lower at 508 K and 2.14 MPa (figure 1(a)) than at 543 K and 0.5 MPa (figure 1(b)) on all catalysts, suggesting that O^* removal as H_2O has a lower activation energy than parallel pathways leading to CO_2.

The slope of the CO_2 selectivity data in figure 1 may also include other secondary routes for the formation of CO_2, such as the conversion of alcohol primary products to acids and their subsequent decarboxylation [18,20]. These pathways are unlikely to contribute appreciably to CO_2 at the conditions of our experiments (508–543 K, 0.5–2.14 MPa, and $H_2/CO = 2$), because alcohol selectivities, and their observed changes with space velocity, are much smaller than the changes in CO_2 selectivity shown in figure 1 and than the changes in alcohol selectivities reported previously at lower H_2/CO ratios (0.7) [18,20]. Water–gas shift reactions, possibly on sites that also catalyze CO dissociation and chain growth as part of FTS catalytic sequences, appear to provide the predominant secondary route for CO_2 formation at the conditions of our experiments.

3.2. *Effects of CO_2 addition to synthesis gas on Fe-based catalysts*

Water–gas shift reactions approach equilibrium with increasing residence time and temperature during FTS (figure 1). This approach to equilibrium and its kinetic consequences can be rigorously described by a parameter η, given by the concentration ratio in equation (1) divided by the equilibrium constant at the reaction temperature:

$$\eta = \frac{1}{K_{\mathrm{WGS}}}\left(\frac{P_{\mathrm{CO_2}}P_{\mathrm{H_2}}}{P_{\mathrm{CO}}P_{\mathrm{H_2O}}}\right). \tag{1}$$

In equation (1), P_j is the partial pressure of species j and K_{WGS} is the WGS equilibrium constant. The value of η ranges from 0 to 1 as chemical reactions approach equilibrium. Figures 3(a) and 3(b) show this value for the two experimental conditions used to obtain the data in figures 1(a) and 1(b). These values suggest that reverse WGS reaction rates are significant. Therefore, the addition of CO_2 to synthesis gas feeds can lead to lower net rates of CO_2 formation and of O^* removal as CO_2 during FTS.

The kinetic consequences of this approach to equilibrium and of the addition of CO_2 can be described by considering how forward rates $r_{\mathrm{f},i}$, and reverse rates $r_{\mathrm{r},i}$, of each elementary step i in the WGS reaction

$$\mathrm{CO} + \mathrm{H_2O} \Leftrightarrow \mathrm{CO_2} + \mathrm{H_2}$$

depend on the affinity of that step (A_i), as given by the De Donder equation [24] of non-equilibrium thermodynamic treatments of chemical kinetics:

$$\frac{r_{\mathrm{f},i}}{r_{\mathrm{r},i}} = \exp\left(\frac{A_i}{RT}\right). \tag{2}$$

The affinity is the negative of the Gibbs free energy of step i:

$$A_i = -\Delta G_i \tag{3}$$

and it is related to standard affinity for that step A_i° by

$$A_i = A_i^\circ + RT\ln\left(\frac{P_{\mathrm{CO_2}}P_{\mathrm{H_2}}}{P_{\mathrm{CO}}P_{\mathrm{H_2O}}}\right). \tag{4}$$

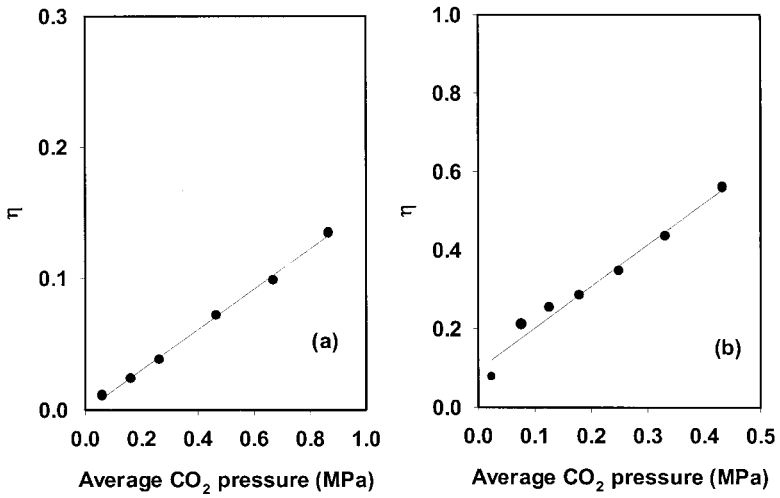

Figure 3. The approach to equilibrium parameter (η) for water–gas shift reaction as a function of the amount of CO_2 added on the $FeZn_{0.1}K_{0.02}Cu_{0.01}$ catalyst; (a) 508 K, 2.14 MPa, $H_2/CO = 2$, and (b) 543 K, 0.5 MPa, $H_2/CO = 2$.

The net rate of the overall reaction is then given by

$$r = r_f - r_b = r_f\left(1 - \exp\left(\frac{-A}{\sigma RT}\right)\right) \quad (5)$$

in which σ is the average stoichiometric number for the catalytic sequence. This number is unity for overall reactions, such as WGS, in which every elementary steps occurs only once in the complete catalytic sequence [25]. Equation (5) then becomes

$$r = r_f - r_r = r_f\left(1 - \exp\left(\frac{-A}{RT}\right)\right). \quad (6)$$

The affinity of the overall reaction (A) depends on the standard reaction affinity A° and on the partial pressures of reactants and products:

$$A = A^\circ + RT \ln\left(\frac{P_{CO_2}P_{H_2}}{P_{CO}P_{H_2O}}\right). \quad (7)$$

The standard affinity A° equals the negative of the standard Gibbs free energies for the reaction and it is related to the equilibrium constant:

$$A^\circ = -\Delta G^\circ = RT \ln K_{WGS}. \quad (8)$$

Combining equations (5) and (6), we obtain

$$A = RT \ln\frac{1}{K_{WGS}}\left(\frac{P_{CO_2}P_{H_2}}{P_{CO}P_{H_2O}}\right) \quad (9)$$

and then from equations (1), (6) and (9) we obtain an expression for the net rate of a chemical reaction as it approaches equilibrium in terms of the parameter η that measures the extent of this approach to equilibrium:

$$r = r_f\left(1 - \frac{1}{K_{WGS}}\left(\frac{P_{CO_2}P_{H_2}}{P_{CO}P_{H_2O}}\right)\right) = r_f(1 - \eta). \quad (10)$$

The forward WGS rate can then be calculated from the measured net rate of CO_2 formation divided by $(1 - \eta)$, where the latter is evaluated at the average partial pressures for each reactant and product in the reactor. The forward rate estimated in this manner is shown in figures 4(a) and 4(b) as a function of CO

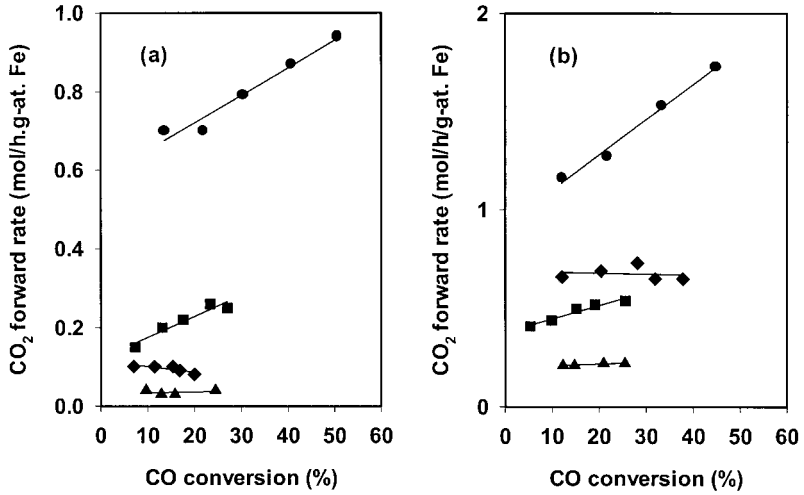

Figure 4. CO_2 forward rate as a function of CO conversion on the different Fe catalysts at (a) 508 K, 2.14 MPa, $H_2/CO = 2$, and (b) 543 K, 0.5 MPa, $H_2/CO = 2$. (▲): $FeZn_{0.1}$, (◆): $FeZn_{0.1}Cu_{0.01}$, (■): $FeZn_{0.1}K_{0.02}$, and (●): $FeZn_{0.1}K_{0.02}Cu_{0.01}$.

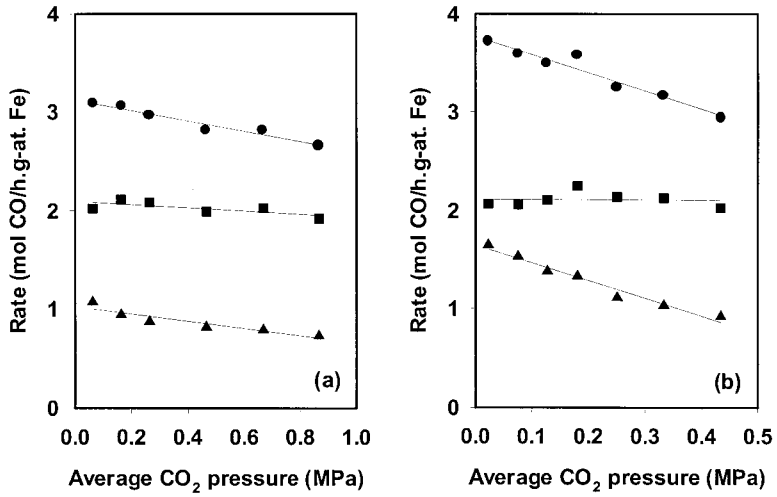

Figure 5. CO conversion rate (●), hydrocarbon formation rate (■) and CO_2 formation rate (▲), as a function of the average CO_2 pressure on the $FeZn_{0.1}K_{0.02}Cu_{0.01}$ catalyst at (a) 508 K, 2.14 MPa, $H_2/CO = 2$, and (b) 543 K, 0.5 MPa, $H_2/CO = 2$.

conversion along with the net CO_2 formation rate for the two reaction conditions used in this study. For the catalysts promoted with K, the CO_2 forward rate increases with increasing conversion, indicating that K increases the rate of the secondary CO_2-forming reactions involving a water co-reactant, which increases in concentration with increasing CO conversion. Cu promotes the removal of O^* by CO^* rather than H^*, but the nearly constant forward CO_2 rate with increasing CO conversion suggests that it does not introduce active sites for secondary water–gas shift reactions. Next, we examine the effects of addition of CO_2 to synthesis gas using this formalism for estimating the effects of CO_2 on the net rate and on the rate of the forward CO_2 formation reactions.

The effects of CO_2 addition on FTS rates and selectivities were examined on $FeZn_{0.1}K_{0.02}Cu_{0.01}$ at the two reaction conditions used for the space velocity data in figure 1 (508 K, 2.14 MPa H_2/CO and 543 K, 0.5 MPa H_2/CO). CO conversion rates and hydrocarbon and net CO_2 formation rates are shown as a function of the average CO_2 pressure in the reactor (the average of the inlet and outlet CO_2 pressures in the reactor) in figures 5(a) and 5(b). The CO conversion rates and the net CO_2 formation rates decreased with increasing CO_2 pressure, but hydrocarbon formation rates were not affected. This shows that the presence of CO_2 in the synthesis gas feed decreases the net rate of CO_2 formation without any influence on the rate of formation of hydrocarbon chains. The effect of CO_2 on the net rate of CO_2 formation is stronger at higher temperatures, apparently because of the faster forward WGS rates and the less favorable equilibrium as temperature increases. The observed decrease in the net rate of CO_2 formation may reflect the inhibition of the forward rate of CO_2-forming reactions or merely an increase in the reverse rate of these reactions as they approach equilibrium. The relative importance of these two effects can be discerned by applying the formalism derived above to these kinetic data.

Figure 6 shows that forward CO_2 formation rates $[r_f = r/(1-\eta)]$ at 543 K are nearly unchanged as the average CO_2 pressure (and hence η) increases. Thus, the presence of CO_2 merely increases the rate of conversion of CO_2 to CO *via* reverse WGS reactions in the exact manner predicted by equation (10). The net rate of CO_2 formation decreases without detectable changes in the rate of the forward reaction and without the appearance of pathways that use CO_2 directly to form hydrocarbons.

Net CO_2 formation rates in figure 6 extrapolate to zero net rates at CO_2 pressures of ~0.85 MPa ($CO_2/CO = 5.5$). At this CO_2 pressure, *all* of the O^* species formed *via* CO dissociation would be removed as H_2O during FTS at 543 K. The required CO_2/CO ratio predicted from equation (10) and the equilibrium constant for WGS at 543 K ($K = 63.6$) is 5.2, in close agreement

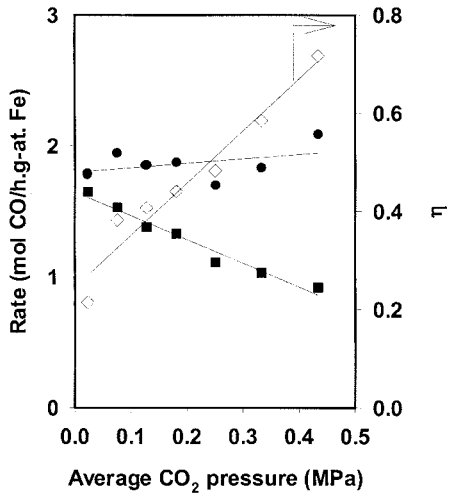

Figure 6. Forward WGS rates (●), net WGS CO_2 formation rates (■), and the approach to equilibrium parameter, η (◇), as a function of CO_2 pressure on the $FeZn_{0.1}K_{0.02}Cu_{0.01}$ catalyst at 543 K, 0.5 MPa, $H_2/CO = 2$.

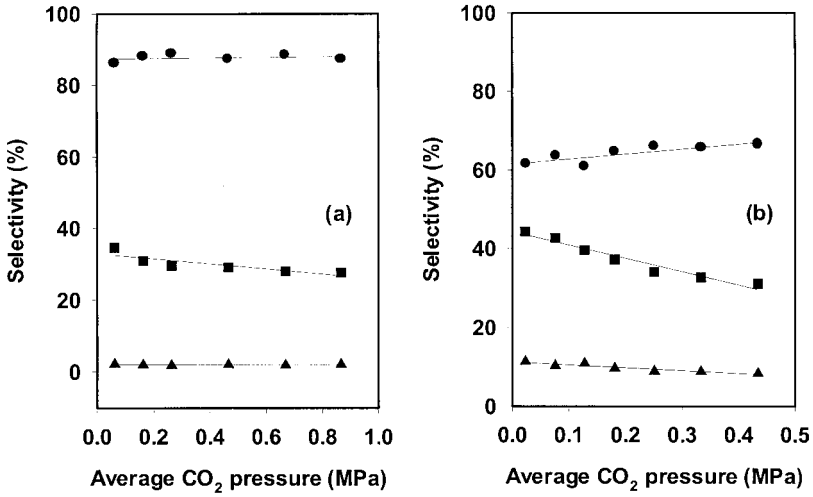

Figure 7. Product selectivities as a function of the average CO_2 pressure on the $FeZn_{0.1}K_{0.02}Cu_{0.01}$ catalyst at (a) 508 K, 2.14 MPa, $H_2/CO = 2$, (b) 543 K, 0.5 MPa, $H_2/CO = 2$; (●): C_{5+}, (■): CO_2 and (▲): CH_4.

with the value of 5.5 obtained from the experimental data shown in figure 6. At 508 K, the effects of CO_2 addition on the net rate of CO_2 formation were much smaller owing to the fact that the WGS reaction was significantly away from equilibrium (figure 2(a)). The use of K_{WGS} values for this temperature and equation (10) leads to a predicted value of ~2.7 MPa ($CO_2/CO = 4.4$).

Net CO_2 selectivities and CH_4 and C_{5+} selectivities (on a CO_2-free basis) are shown as a function of the average CO_2 pressure in figures 7(a) and 7(b) for the two reaction conditions used in these experiments. At 543 K, CO_2 leads to a slight increase in C_{5+} selectivity and to a concomitant decrease in CH_4 selectivity (figure 7(b)); these effects are not detectable at lower temperatures (figure 7(a)). These selectivity effects appear to reflect small changes in the H_2/CO usage ratio as the O^* is increasingly removed as water (using H_2) instead of CO_2 (using CO) as the CO_2 concentration increases. They lead to slightly lower average H_2/CO ratios throughout the catalyst bed (figures 8(a) and 8(b)), especially at higher temperatures, for which oxygen removal selectivities depend on the presence and concentration of CO_2 in the synthesis gas. H_2 and CO chemisorption are generally assumed to be quasi-equilibrated during FTS [26]; therefore, these changes in the H_2/CO ratio lead to a concomitant increase in the surface coverages of CO^* relative to H^* and to an increase in the probability of chain growth and in the average molecular weight of the products formed. These changes become detectable only at higher temperatures, for which significant reverse rates lead to appreciable changes in the synthesis gas composition. The α-olefin/n-paraffin ratios on $FeZn_{0.1}K_{0.02}Cu_{0.01}$ also increase with increasing CO_2 pressure (figures 8(a) and 8(b)) for chains of all sizes at 543 K, while the effects were very small at 508 K. These changes are also

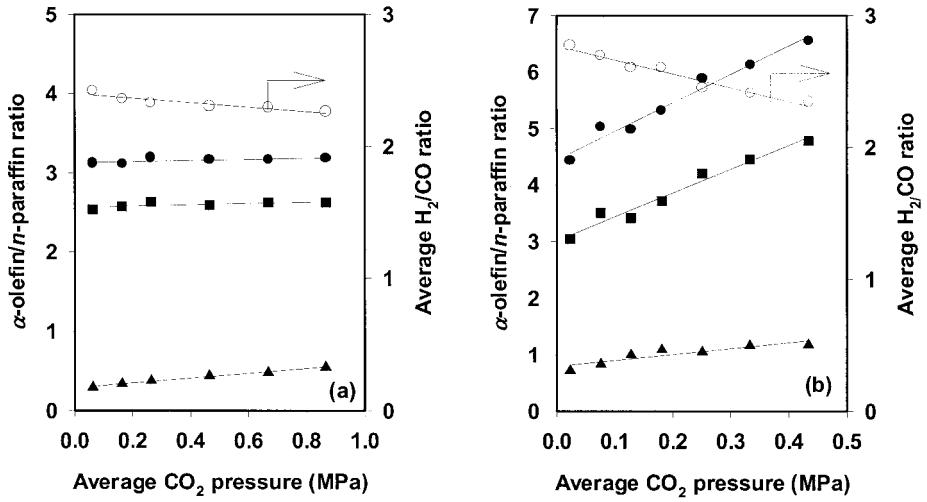

Figure 8. α-Olefin/n-paraffin ratio for different hydrocarbon chain sizes as a function of the average CO_2 pressure on the $FeZn_{0.1}K_{0.02}Cu_{0.01}$ catalyst at (a) 508 K, 2.14 MPa, and (b) 543 K, 0.5 MPa, $H_2/CO = 2$; (●): C_3H_6/C_3H_8, (■): $1\text{-}C_5H_{10}/n\text{-}C_5H_{12}$, (▲): $1\text{-}C_1H_{22}/n\text{-}C_{11}H_{24}$, and (○): average H_2/CO ratio in the reactor.

consistent with the lower H_2/CO ratios and the lower expected surface H^* concentrations prevalent when CO_2 is added to the synthesis gas stream.

These results show that the extent to which O^* is removed as CO_2 during FTS can be controlled by the addition or recycle of CO_2 and that the required CO_2 concentrations can be accurately estimated using a rigorous kinetic treatment of reversible reactions as such reactions approach equilibrium. At temperatures and reaction conditions for which WGS reactions are far away from equilibrium, the complete inhibition of CO_2 formation requires large CO_2/CO ratios. However, at higher temperatures, which lead to higher forward WGS rates and to less favorable WGS thermodynamics, the CO_2/CO ratios required to eliminate CO_2 formation become small enough for potential use of CO_2 recycle when H_2/CO mixtures derived from natural gas are used on Fe-based FTS catalysts.

3.3. *The role of CO_2 in the initiation and growth of hydrocarbon chains*

As WGS reactions approach equilibrium during FTS, CO and CO_2 become kinetically indistinguishable, because their interconversion is much faster than the chain initiation and growth steps required for hydrocarbon formation. Then, a significant fraction of the C-atoms in CO_2 can contribute towards the formation of hydrocarbons, but *via* the formation of CO intermediates in reverse WGS reactions. A direct role of CO_2 in chain initiation and propagation was proposed by Xu *et al.* [18,21], but it is unclear how such conclusions could be reached from isotopic experiments influenced by significant chemical (and isotopic) interconversion of CO and CO_2 *via* WGS reactions.

Table 1
Conditions for $^{13}CO_2$ addition experiments performed on the $FeZn_{0.1}K_{0.04}Cu_{0.02}$ catalyst, reaction parameters and ^{13}C content in different components

Temperature (K)	508
Synthesis gas pressure (MPa) ($H_2/CO = 2$)	0.8
$^{13}CO_2$ pressure (MPa)	0.1
CO conversion (%)	21.1
CO_2 selectivity (%)	35.9
η [a]	0.025
Selectivity (CO_2-free, %) CH_4	3.5
Selectivity (CO_2-free, %) C_{5+}	81.8

[a] As defined in equation (1).

Here, we report the results of experiments in which 0.1 MPa $^{13}CO_2$ was added to synthesis gas ($P_{CO} = 0.25$ MPa, $P_{H_2} = 0.50$ MPa and $P_{N_2} = 0.05$ MPa) at conditions far removed from the WGS equilibrium ($\eta = 0.025$). The CO conversion and product selectivities are listed in table 1. The ^{13}C contents in hydrocarbon chains of a given size were measured in order to probe the relative contributions of $^{13}CO_2$ and ^{12}CO to chain initiation and chain growth. These results were not corrupted by any isotopic or chemical equilibration between the CO and CO_2 components in the reactant stream. As shown in figure 9, the ^{12}CO reactant exiting the reactor retains the ^{12}C isotopic purity, while the initially pure $^{13}CO_2$ reactants retain ^{13}C fractions greater than 0.5.

The ^{13}C contents in CO_2, CO, hydrocarbons and oxygenates (aldehydes + alcohols) are shown in figure 9. No ^{13}C was detected in CO, suggesting that dilution of the CO reactant by CO molecules formed from CO_2 *via* reverse WGS reactions was negligible at these reaction conditions, consistent with the low value of η

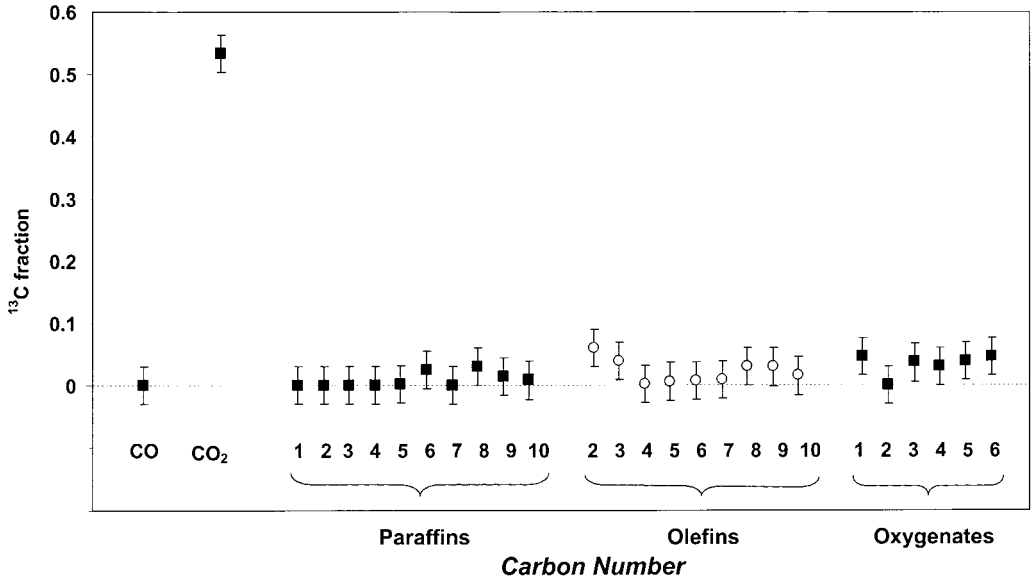

Figure 9. ^{13}C fraction in CO, CO_2, paraffins, olefins and oxygenates during $^{13}CO_2$ addition runs on the $FeZn_{0.1}K_{0.04}Cu_{0.02}$ catalyst at 508 K, 0.8 MPa, $H_2/CO = 2$, 0.1 MPa $^{13}CO_2$.

(= 0.025). The fraction of ^{13}C in CO_2 was 0.533, because CO_2 formed during O^* removal using CO or *via* WGS reactions dilutes the isotopically pure $^{13}CO_2$ reactants. The ^{13}C fraction in all C_1–C_{10} paraffins, C_2–C_{10} olefins, and C_1–C_8 oxygenates are much lower than in CO_2, and in most cases, well below the detection limit (~0.02–0.03) of our analytical methods. Clearly, no preferential incorporation of CO_2 is detected in any of the hydrocarbon products; exclusive chain initiation by CO_2, as proposed earlier [18,21], would have led to significant isotopic enrichment of the smaller products and to a decrease in the ^{13}C content with increasing chain size, neither of which was experimentally observed in our study (figure 9). Also, the reactivity of CO_2 in chain initiation and growth would have to be at least five times lower than that of CO, because the average ^{13}C fraction in the combined CO/CO_2 pool is about 0.25, while that in the pool of hydrocarbon formed is less than 0.05, and for most of the hydrocarbons below the detection limit. Thus, the participation of CO_2 is no greater than that of CO in either the formation of monomers or the initiation of chains, and probably much smaller. CO_2 is also not involved in alcohol formation, because the ^{13}C content in alcohols was also very low and similar to that found in hydrocarbons.

4. Conclusions

An investigation of the CO_2 formation and reaction pathways during Fischer–Tropsch synthesis (FTS) has been carried out on a co-precipitated Fe–Zn catalyst promoted with Cu and K. The removal of adsorbed oxygen formed during CO dissociation steps can occur by primary and secondary pathways. Primary pathways for oxygen removal include reactions with adsorbed hydrogen to form H_2O and with adsorbed CO to form CO_2. The relative probability of oxygen removal either as H_2O or CO_2 is determined by the reaction temperature and the presence of promoters (Cu and K). H_2O formed by primary pathways can undergo readsorption followed by its subsequent reaction with CO-derived intermediates leading to the formation of CO_2. The forward rate of CO_2 formation increases with an increase in residence time, while the net CO_2 formation rate decreases due to the approach towards WGS reaction equilibrium. CO_2 addition during FTS does not influence CO_2 forward rates, but increases the rate of their reverse steps leading to the attainment of WGS equilibrium; and hence it can result in the minimization of CO_2 formation during FTS and the preferential removal of oxygen as H_2O. CO_2 addition also results in lower H_2/CO ratios in the reactor, which in turn resulted in higher C_{5+} selectivities and olefin content. From our experimental data and the predictions from our thermodynamic treatment, it was found that at 543 K, the addition of 0.85 MPa CO_2 to synthesis gas ($H_2/CO = 2$, 0.50 MPa) could eliminate CO_2 formation during FTS and lead to the complete removal of dissociated oxygen formed during FTS as H_2O. These studies also suggest that the recycle of CO_2 formed during FTS can be used as a tool to improve the carbon efficiency on Fe catalysts, which in turn adds to their advantage of being cheaper and more flexible than Co catalysts. Finally, the addition of $^{13}CO_2$ to $H_2/^{12}CO$ reactants showed that the hydrocarbon products had a negligible ^{13}C content, indicating that CO_2 is much less reactive than CO towards chain initiation and growth. Our studies also show that except at WGS reaction equilibrium, where CO and CO_2 become kinetically indistinguishable from each other, CO_2 does not appear to compete with CO towards chain initiation and growth reactions.

Acknowledgments

We would like to acknowledge the financial support provided by the U.S. Department of Energy (DE-FC26-98FT40308) for this work.

References

[1] F. Fischer and H. Tropsch, Brennstoff-Chem. 7 (1926) 97.
[2] R.B. Anderson, *The Fischer–Tropsch Synthesis* (Academic Press, Orlando, FL, 1984).
[3] M.E. Dry, *The Fisher–Tropsch Synthesis*, in: *Catalysis—Science and Technology*, Vol. 1, eds. J.R. Anderson and M. Boudart (Springer, New York, 1981), p. 160.
[4] H.H. Storch, N. Golumbic and R.B. Anderson, *The Fischer–Tropsch and Related Syntheses* (Wiley, New York, 1951).
[5] M.A. Vannice, in: *Catalysis—Science and Technology*, eds. J.R. Anderson and M. Boudart (Springer, Berlin, 1982), p. 139; M.A. Vannice, Catal. Rev. Sci. Eng. 3 (1976) 153.
[6] S. Li, A. Li, S. Krishnamoorthy and E. Iglesia, Catal. Lett. 77(4) (2001) 197.
[7] S. Li, S. Krishnamoorthy, A. Li, G.D. Meitzner and E. Iglesia, J. Catal. in press.
[8] S. Li, G.D. Meitzner and E. Iglesia, J. Phys. Chem. B 105 (24) (2001) 5743.
[9] S.L. Soled, E. Iglesia, S. Miseo, B.A. DeRites and R.A. Fiato, Topics Catal. 2 (1995) 193.
[10] A.P. Raje, R.J. O'Brien and B.H. Davis, J. Catal. 180 (1998) 36.
[11] D. Newsome, Catal. Rev. Sci. Eng. 21 (2) (1980) 275.
[12] D.C. Grenoble, M.M. Estadt and D.F. Ollis, J. Catal. 67 (1981) 90.
[13] D.G. Rethwisch and J.A. Dumesic, J. Catal. 101 (1986) 35.
[14] E.S. Lox and G.F. Froment, Ind. Eng. Chem. Res. 32 (1993) 71.
[15] K.R.P.M. Rao, F.E. Huggins, V. Mahajan, G.P. Huffman, V.U.S. Rao, B.L. Bhatt, D.B. Bukur, B.H. Davis and R.J. O'Brien, Topics Catal. 2 (1995) 71.
[16] G.P. Van der Laan and A.A.C.M. Beenackers, Appl. Catal. A 193 (2000) 39.
[17] W.K. Hall, R.J. Kokes and P.H. Emmett, J. Am. Chem. Soc. 82 (1960) 1027.
[18] L. Xu, S. Bao, L.-M. Tau, B. Chawla, H. Dabbagh and B.H. Davis, 11th Annual International Pittsburgh Coal Conference Proceedings, p. 88, 1994.
[19] W.K. Hall, R.J. Kokes and P.J. Emmett, J. Am. Chem. Soc. 79 (1957) 2983.
[20] B.H. Davis, L. Xu and S. Bao, *Natural Gas Conversion IV*, Stud. Surf. Sci. Cat. 107 (1997) 175.

[21] L. Xu, S. Bao, D.J. Houpt, S.H. Lambert and B.H. Davis, Catal. Today 36 (1997) 347.
[22] G. Price and E. Iglesia, Ind. Eng. Chem. Res. 28(6) (1989) 839.
[23] T. Utaka, K. Sekizawa and K. Eguchi, Appl. Catal. A 194–195 (2000) 21.
[24] T. De Donder, *L'affinité* (Gauthier-Villars, Paris, 1927).
[25] M. Boudart and G. Djega-Mariadassou, *Kinetics of Heterogeneous Catalytic Reactions, Physical Chemistry: Science and Engineering* (Princeton University Press, Princeton, 1984).
[26] A. Li and E. Iglesia, unpublished results.